

# Quantum Circuit Placement: Optimizing Qubit-to-qubit Interactions through Mapping Quantum Circuits into a Physical Experiment

**D. Maslov**  
 Institute for Quantum Computing  
 University of Waterloo  
 Waterloo, ON, N2L 3G1, Canada  
 dmitri.maslov@gmail.com

**S. M. Falconer**  
 Department of Computer Science  
 University of Victoria  
 Victoria, BC, V8W 3P6, Canada  
 seanf@uvic.ca

**M. Mosca**  
 Institute for Quantum Computing  
 University of Waterloo  
 Waterloo, ON, N2L 3G1, Canada  
 mmosca@iqc.ca

March 10, 2019

## Abstract

We study the problem of the practical realization of an abstract quantum circuit when executed on quantum hardware. By practical, we mean adapting the circuit to particulars of the physical environment which restricts/complicates the establishment of certain direct interactions between qubits. This is a quantum version of the classical circuit placement problem. We study the theoretical aspects of the problem and also present empirical results that match the best known solutions that have been developed by experimentalists. Finally, we discuss the efficiency of the approach and scalability of its implementation with regards to the future development of quantum hardware.

## 1 Introduction

Quantum algorithm design is usually done in an abstract model of computation with the primary interest being the development of *efficient* algorithms (e.g. polynomial versus exponential sized circuits) independently of the details of the potential physical realization of the related quantum circuits. Theoretical quantum computational architectures usually, for convenience, assume that it is possible to directly interact any two physical qubits. It is well known that in physical implementations<sup>1</sup> direct interactions between two distinct qubits may sometimes be hard if not impossible to establish. For instance, it is not uncommon for an interaction to have less than 0.2 Hz frequency (e.g. carbons C2 and C6 from [16]), while the decoherence may take around one second. This means that the interaction between such qubits will be essentially seen as noise. A physical realization of a quantum processor can of course *indirectly* couple any two qubits, with some overhead cost. However, in practice this can be very costly (and, for example, make the implementation infeasible with available technology), and so one needs to find a way to minimize this overhead, which we further refer to as quantum circuit placement problem.

Some authors [14] try to avoid long interactions by considering the linear nearest neighbor computational architecture where all qubits are lined up in a chain (such as trapped ions [7]) and only the nearest neighbors are allowed to interact. Mathematically, for a system with  $n$  qubits  $q_1, q_2, \dots, q_n$ , the 2-qubit gates are allowed on qubits whose subscript values differ by one. Such an architecture, however, *does not necessarily* represent reality. For instance, in NMR technologies the fastest interactions will not usually form a chain. In a 3-qubit computation, the fastest interactions can be aligned to form a chain (acetyl chloride, Figure 1, [12]) or a complete graph [5]. In all molecules used in NMR and known to the authors that employ four or more qubits, the fastest interactions are established along the chemical bonds and they do not form a single chain. The chain nearest neighbor architecture can apply to some quantum dot based architectures and certain variations of trapped ion

<sup>1</sup> Trapped ions [7] and liquid NMR (Nuclear Magnetic Resonance) [4] are two of the most developed quantum technologies targeted for computation (as opposed to communication or cryptography). Other state of the art quantum information processing proposals are described in [8].

[7] quantum technologies, but does not represent the reality behind other technologies, including those based on NMR, Josephson junctions, optical technology, and certain other variations of trapped ions [15]. Furthermore, we are unaware of any automated procedure for optimizing the interactions even if the latter are restricted to the chain nearest neighbor architecture.

It has been recently proposed to use EPR pairs to teleport logic qubits in a Kane model when long-distance swapping of a *single* value becomes too expensive [2]. However, this type of “technology mating” may not always be possible. For instance, it seems hard if not impossible to mate NMR with an optic EPR source while doing a computation on an NMR machine. It is not obvious how congested such an architecture gets if simultaneous teleporting of a large number of qubits is required. We concentrate on an approach that does not require mating different technologies, and is *technology independent*.

Unlike in the quantum case, the classical circuit placement problem is very well known and extensively studied [13]. Classical circuit placement is concerned primarily with minimizing the total wirelength, power, and congestion. Timing minimization is considered to be a secondary optimization objective. In quantum technologies, placement is equivalent to timing optimization under the natural assumption that gate fidelities [17] are inversely proportional to the coupling strength/gate runtime, otherwise, a function of both may be considered. However, timing minimization for quantum versus CMOS technologies are two distinct and dissimilar problems. This is not surprising given the conceptual differences in the two computational models. A quantum circuit placer cannot be constructed by reusing the existing EDA tools and thus, must be built from scratch.

In practice and at present, the mapping of qubits in a circuit into physical qubits is done by hand, but as the quantum computations scale, a more robust (automated) technique for such a mapping must be employed. In this paper, we study the problem of mapping a circuit into a physical experiment where we wish to optimize the interactions. We formulate this problem mathematically and study its complexity. Given the problem of finding an optimal assignment of qubits is unlikely to have a polynomial time optimal solution, as it is NP-Complete, and exhaustive search requires  $n!$  tries for an  $n$ -qubit system, we develop a heuristic-based algorithm. We verify the latter on data taken from existing quantum experiments.

Throughout the text, and especially in the experimental results section, we refer to liquid state NMR technology for quantum computation. While there are certain problems with using liquid state NMR to work with over 10 qubits [4, 9, 16], so far, it is the best developed methodology for quantum computing experiments. Liquid state NMR experiments provide a nice data set for both the interaction frequencies and the circuits of interest, and a test bed for development of suitable scalable spin-based quantum computing devices. While we use results from the liquid state NMR experiments, it is important to emphasize that our approach is not restricted to a particular technology.

## 2 Preliminaries

We present a short review of the basic concepts of quantum computation. For a more detailed introduction, please see [17].

The state of a single qubit is a linear combination  $\alpha|0\rangle + \beta|1\rangle$  (also written as a vector  $(\alpha, \beta)$ ) in the basis  $\{|0\rangle, |1\rangle\}$ , where  $\alpha$  and  $\beta$  are complex numbers called the amplitudes, and  $|\alpha|^2 + |\beta|^2 = 1$ . Real numbers  $|\alpha|^2$  and  $|\beta|^2$  represent the probabilities  $p$  and  $q$  of reading the “pure” logic states  $|0\rangle$  and  $|1\rangle$  upon measurement. The state of a quantum system with  $n > 1$  qubits is given by an element of the tensor product of the single state spaces and can be represented as a normalized vector of length  $2^n$ , called the state vector. Quantum system evolution allows changes of the state vector through its multiplication by  $2^n \times 2^n$  unitary matrices.

The above models how a transformation can be performed, but does not indicate how to identify the unitary matrices that compose the transformation or how to implement them. Typically, certain primitive gates are used as elementary building blocks. In practice, elementary gates are defined by the form of the Hamiltonian, the latter depends on a particular implementation/technology. While our placement algorithms/theory and program implementation *readily support any gate library*, we next introduce some of the particular gates used in the examples included in this paper. In liquid state NMR technology elementary gates are [4]:

- rotation gates  $R_x(\theta) := \begin{pmatrix} \cos(\frac{\theta}{2}) & -i\sin(\frac{\theta}{2}) \\ -i\sin(\frac{\theta}{2}) & \cos(\frac{\theta}{2}) \end{pmatrix}$ ,  $R_y(\theta) := \begin{pmatrix} \cos(\frac{\theta}{2}) & -\sin(\frac{\theta}{2}) \\ \sin(\frac{\theta}{2}) & \cos(\frac{\theta}{2}) \end{pmatrix}$ , and  $R_z(\theta) := \begin{pmatrix} e^{-i\theta/2} & 0 \\ 0 & e^{i\theta/2} \end{pmatrix}$ ;

- two qubit interaction gate

$$ZZ(\theta) := \begin{pmatrix} e^{-i\theta/2} & 0 & 0 & 0 \\ 0 & e^{i\theta/2} & 0 & 0 \\ 0 & 0 & e^{i\theta/2} & 0 \\ 0 & 0 & 0 & e^{-i\theta/2} \end{pmatrix}.$$

Physically, single qubit  $R_x$  and  $R_y$  gates are implemented by RF pulses in the  $X$ - $Y$  plane.  $R_z$  gates can be implemented by the change of the rotating reference frame and thus require no action/waiting. Finally,  $ZZ$  gates are a part of the drift Hamiltonian and must be waited for until completion. Note that  $ZZ(\pi/2)$  is equivalent to CNOT up to the single qubit rotations. This means that every circuit with a single qubit and CNOT gates can be easily rewritten in terms of single qubit rotations and  $ZZ(\pi/2)$ , and such an operation does not change a particular instance of the placement problem.

### 3 Formalization of the circuit mapping problem

Circuits devised by researchers in the area of quantum computing are very often written in terms of a single qubit and two qubit gates. Thus, any circuit with gates spanning over more than two qubits is first translated into a circuit with a single qubit and two qubit gates. We assume such a circuit as input. Next, most of the practical circuits are levelled, that is the gates that can be applied in parallel appear at one logic level (in circuit diagrams: directly below or above other gates from the same level). Levelization helps to reduce the overall runtime of the circuit, and thus it is a desired operation at the time the circuit is synthesized.

Before the circuit's qubits are mapped into molecule's nuclei and the exact delays are known, it is hard to decide how long it will take to execute a single gate and take it into account while trying to minimize the delay of the entire circuit. This means that the circuit's qubits must be mapped to the molecule's nuclei first.

In a practical setting and according to how it is done in current experiments the *first* step is to efficiently assign qubits to nuclei. In the existing NMR tools, the timing optimization is built into a compiler [1] that takes in a circuit and a refocusing scheme and outputs a sequence of (timed) pulses ready to be executed. This is the last step before the circuit gets executed and before it is done the logical qubits must be assigned to the nuclei.

In practice, it is a natural assumption that gates from the next level can start being executed before execution of the current level has completed. The total **runtime** is defined as the time spent by a circuit between the input initialization and measurement of the output. With the assumptions made, runtime of a circuit composed of gates  $G[1], G[2], \dots, G[k]$  can be found by the following dynamic programming algorithm.

```

Create array Time[1..n] and initiate its elements to 0;
for i=1..k
    if G[i] is a two-qubit gate built on qubits t and c
        time[c]:=max{time[c],time[t]}+GateOperatingTime(G[i]);
        time[t]:=time[c];
    else // else means gate G[i] is a single qubit gate
        // that operates on qubit t
        time[t]:=time[t]+GateOperatingTime(G[i]);
    end if;
end for;
return max{time[1..n]}; // maximally busy qubit is the
                        // one that finishes the job last

```

Circuit runtime calculation in a computational model where logic levels need to be executed sequentially is also supported by the theory we develop and our program implementation. We next introduce the following notations/definitions.

**Definition 1.** A **physical environment (molecule)** is a complete non-oriented graph with a finite set of vertices (nuclei)  $\{v_1, v_2, \dots, v_m\}$  and weighted edges  $\{(v_i, v_j)\}_{1 \leq i \leq j \leq m}$  with  $W(v_i, v_j) \geq 0$ .

Weights  $W(v_i, v_j)$  are proportional to the inverse of the coupling frequency (for two qubit gates) and the inverse of nuclei processing frequencies (for single qubit gates). In other words, they indicate how long it takes to apply a fixed angle 2-qubit gate (in case of edge  $(v_i, v_j)$ ,  $i \neq j$ ) or a fixed angle single qubit gate (in case of edge  $(v_i, v_i)$ ).

**Definition 2.** A quantum circuit is built on  $n$  qubits  $q_1, q_2, \dots, q_n$  and consists of a finite number of levels  $L_1, L_2, \dots, L_k$ , where each level  $L_i$  is a set of one or two qubit gates  $G_i^1, G_i^2, \dots, G_i^{l_i}$ . Each gate has a weight function  $T(G_i^j)$  that indicates how long it takes this gate to use the interaction defined by the bits it operates on<sup>2</sup>.

**Definition 3.** The quantum circuit placement problem is to construct an injective (one-to-one) function  $P : \{q_1, q_2, \dots, q_n\} \mapsto \{v_1, v_2, \dots, v_m\}$  such that with this mapping the runtime of a given circuit is minimized. The gate's  $G(v_i, v_j)$  execution cost is defined by the mapping  $q_i \mapsto v_i$ ,  $q_j \mapsto v_j$  according to the formula  $\text{GateOperatingTime}(G(q_i, q_j)) := W(v_i, v_j) * T(G(q_i, q_j))$ .

There are  $\frac{m!}{(m-n)!}$  potential candidates for an optimal matching.

**Example 1.** Illustrated in Figure 1(a) is acetyl chloride molecule and a table with the chemical shifts/coupling strengths (in liquid state NMR) [12]. The chemical shifts and coupling strengths were recalculated into the delays needed to apply 90-degree rotations in the X-Y plane (single qubit rotations with respect to axis Z are “free” in that they are done by changing the rotating reference frame [11] and require no pulse or a delay associated with respect to their application [4]) and a 90-degree zz-rotation (2 qubit gate). The delays are measured in terms of  $\frac{1}{10000}$  sec, and are rounded to keep the numbers as an integer. Figure 1(b) describes liquid state NMR computational properties of the molecule in graph form.

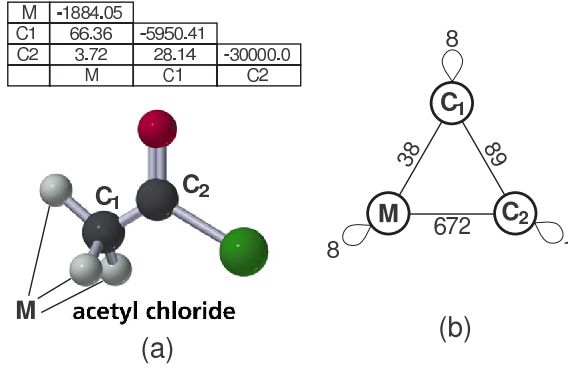


Figure 1: (a) acetyl chloride molecule with three spin- $\frac{1}{2}$  nuclei used as qubits:  $M$  (three hydrogens that share the same chemical environment and thus appear practically indistinguishable),  $C_1$  and  $C_2$  (both are carbons) and (b) graph representation of interactions between qubit nuclei of this molecule.

**Example 2.** Illustrated in Figure 2 is a circuit (in terms of NMR pulses) for the encoding part of the 3-qubit quantum error correction code taken from [12]. It consists of a number of single qubit and two qubit gates. Gates  $R_y(90)$  require an RF pulse of the length proportional to the degree of rotation. Since the degree of rotation is 90,  $T(R_y(90)) = 1$ . In liquid state NMR gates  $R_z(90)$  and  $R_z(-90)$  can be applied through the change of rotating reference frame and require no delay. Thus,  $T(R_z(90)) = T(R_z(-90)) = 0$ . Both zz-interactions are 90-degree, therefore  $T(ZZ(90)) = 1$ .

**Example 3.** Let us consider the placement problem of the 3-qubit encoding quantum circuit (Figure 2) into acetyl chloride (Figure 1). There are  $3! = 6$  possible placement assignments. One possible placement is the following:  $a \rightarrow M$ ,  $b \rightarrow C_2$  and  $c \rightarrow C_1$ . The circuit runtime calculation is illustrated in Table 1 for steps  $i = 1..5$  appearing in columns 2-6 and the first column listing the available qubits. Single qubit rotations around Z axis are ignored since their contribution to the runtime is zero. The circuit runtime equals the largest number in the last column,

<sup>2</sup>For example,  $T(R_x(180)) = 2 * T(R_x(90))$  because it takes twice the time to do a 180-degree rotation as compared to a 90-degree rotation.

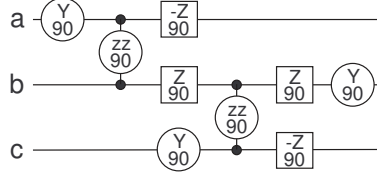


Figure 2: Encoding part of the 3-qubit error correcting code.

770. This example placement is not optimal. The minimal possible value of runtime is equal to 136, and is achieved by the placement  $a \rightarrow C_2$ ,  $b \rightarrow C_1$ ,  $c \rightarrow M$ .

time[]	$Y_a 90$	$ZZ_{ab} 90$	$Y_c 90$	$ZZ_{bc} 90$	$Y_b 90$
a	8	680	680	680	680
b	0	680	680	769	770
c	0	0	8	769	769

Table 1: Cost of  $\{a \rightarrow M, b \rightarrow C_2, c \rightarrow C_1\}$  mapping.

## 4 Complexity

In this section we show that the placement problem is NP-Complete, and thus we need to focus on heuristic solutions. In particular, we consider the problem of finding a Hamiltonian cycle in a graph  $H = (V_H, E_H)$ . We next formulate a mapping problem whose solution is equivalent to the solution of a Hamiltonian cycle problem.

Let the physical environment be a graph with the same set of vertices as graph  $H$ ,  $\{v_1, v_2, \dots, v_m\}$ . Edge  $(v_i, v_j)$  of the physical environment has weight one if and only if  $(v_i, v_j)$  is not an edge of graph  $H$ . All other edges have weight zero. The physical environment, as defined, models the graph  $H$  from the Hamiltonian cycle problem. Let the quantum circuit consist of  $m$  levels and be built on  $m$  qubits  $\{q_1, q_2, \dots, q_m\}$ . Let the  $i^{\text{th}}$  level be composed of a single 2-qubit gate  $G(q_i, q_{(i \bmod m)+1})$  with  $T(G) = 1$ . Runtime of the circuit is thus the sum of the execution runtimes of its gates. The defined quantum circuit models the Hamiltonian cycle. When the quantum circuit is mapped into the physical environment such that its runtime is minimized, the minimal possible value of runtime, which is zero, is possible to achieve if and only if the physical environment has a Hamiltonian cycle that goes along the edges with zero weight. This is equivalent to  $H$  having a Hamiltonian cycle.

## 5 Heuristic solution

Before we begin the description of our algorithm, we first make several observations about qubit assignment. Firstly, in real world experiments, such as [10, 16], the qubit-to-qubit interactions are usually aligned along the chemical bonds, or otherwise using only the fastest interactions allowed by the physical environment. Secondly, most often a single qubit gate can be executed much faster than a two-qubit gate. Third, it may turn out that a circuit is composed of a number of computations/stages each of which has its own best mapping into a physical environment. If the circuit is treated as a whole, no placement will be efficient because at least one part of such a placement will be inefficient. Below, we describe an approximate placement algorithm that uses heuristics derived from these observations.

### 5.1 Algorithm

**Preprocessing.** We first take the physical environment and establish which interactions are considered the fastest. One method for doing this is to choose a *Threshold* such that if a value of a qubit-to-qubit interaction is below

the *Threshold*, the interaction is considered to be fast, otherwise it is considered too slow and will not be used. The value of the *Threshold* may be chosen to be the minimal value such that the graph associated with fastest interactions is connected, or may be taken directly from the experimentalists. Either way, we treat the value of the *Threshold* as a known parameter for our algorithm. Using the *Threshold* value insures that our algorithm comes up with a circuit implementation that uses only the fastest interactions.

**Body.** The algorithm consists of two stages: basic placement and fine tuning, repeated iteratively. In the basic mapping stage we make sure that in some part of the circuit all two qubit gates can be aligned along the fastest interactions of the physical environment. In the fine tuning stage we consider a given subcircuit for which a mapping of circuit qubits into the molecule's nuclei along the fastest interactions exists. We fine tune this matching by shuffling the solution and taking the actual numbers that represent the length of each gate (including single qubit gates) into account.

We start by reading in the 2-qubit gates from the circuit into a workspace  $C$  and do it as long as these gates can be arranged along the fastest interactions provided by the physical environment. As soon as we reach a gate whose addition will prohibit the alignment along the fastest interactions, we stop and concentrate on those gates already in  $C$ . At this point, we know that the two qubit gates we have read,  $g_1, g_2, \dots, g_s$ , can be aligned along the fastest interactions. Take one of such alignments in the case when multiple alignments are possible. The alignment itself can be found by any of the known graph monomorphism techniques, such as [3]. If all monomorphisms can be found reasonably fast (which is true for all experimentally constructed circuits and environments we tried due to their small size), we calculate the circuit runtime for each of them and take the best found. Otherwise, we apply a simple hill climbing algorithm, where for every qubit  $q_i$  from the circuit such that there exists a two qubit gate  $g_j$  among those in  $C$  that operates on this qubit, try to map it to any of  $\{v_1, v_2, \dots, v_m\}$  and see if this new placement assignment is better than the one provided by the initial matching. If it is, change the way qubit  $q_i$  is placed, otherwise, move on to the next qubit. Such an operation can be repeated until no improvement can be found or for a set number of iterations. We refer to this step as fine tuning. After the matching is fine tuned, we return to the circuit, erase all the gates from it up to the two qubit gate  $g_{s+1}$  that prevented alignment along the fastest interactions at the previous step and repeat the above procedure.

The result of the above algorithm is a finite set of finely tuned placement assignments  $P_1, P_2, \dots, P_t$ , but they apply to different subcircuits  $C_1, C_2, \dots, C_t$  of the target circuit. The overall computation looks as follows  $C_1 E_{1,2} C_2 E_{2,3} \dots E_{t-1,t} C_t$ , where  $E_{i,i+1}$  is a circuit composed with SWAP gates such that  $E_{i,i+1}$  transforms mapping given by  $P_i$  into the mapping given by  $P_{i+1}$ , and initially all qubits are placed according to  $P_1$ .

## 5.2 Fast permutation circuits

The algorithm from the previous subsection describes all details of the circuit placement, except how to construct circuits  $E_{i,i+1}$  that would swap the placement assignment of subcircuit  $C_i$  into that for  $C_{i+1}$ . In this subsection we discuss how to compose such circuits efficiently (linear in number of qubits in the physical environment; and using only the fastest interactions) and solely in terms of SWAP gates.

**Problem.** For a given permutation (defined as the permutation transforming placement assignment of subcircuit  $C_i$  into that for  $C_{i+1}$ ) and a graph defining which two qubits can be interchanged through a single SWAP (such an *adjacency graph* has an edge between two qubits if it is possible to SWAP their values directly, meaning that the interaction between the two qubits is considered fast) compose a set of SWAPs that realize this permutation.

**Observations.** Note that the interaction graph is connected.

**Assumptions.** For simplicity, we assume that all SWAP gates applied to the qubits joined by the edges of adjacency graph  $G$  require the same time. Modification of the algorithm presented below that accounts for the actual costs of SWAPs is possible, but it is not discussed here. Next, assume that the graph  $G$ , as well as its subgraphs, are *well separable*. That is, there exists a constant  $s \in (0, 1)$  such that  $G$  can be recursively divided into two connected components  $G_1$  and  $G_2$ , and the ratio of the number of vertices in the smaller subgraph to the number of vertices in the larger subgraph is never less than  $s$ . This is certainly true for the scalable interaction architectures proposed in the literature: linear nearest neighbor architecture (1D lattice,  $s = 1/2$ ), and 2D lattices ( $s \geq 1/2$ ). In our experiments, we found that the interaction graphs for liquid state NMR molecules have  $s = 1/2$ .

If a number of pairs with different values is to be swapped, the runtime of the experimental implementation of such an operation is associated with the cost of a single SWAP. We make this assumption because in quantum

technologies it is possible (not prohibited, and often explicitly possible, such as in liquid state NMR) to execute non-intersecting gates in parallel.

**Goal.** Our target is to minimize the number of logic levels one needs in order to realize a given permutation as a circuit. Each logic level is composed with a set of non-intersecting SWAPs operating along the fastest interactions defined by the adjacency graph.

**Solution.** Consider adjacency graph  $G$  with  $n$  vertices that shows which SWAPs can be done directly. Cut this graph into two connected subgraphs  $G_1$  and  $G_2$  with the number of vertices equal to or as close to  $n/2$  as possible. To do such a cutting we would have to cut a few edges, each called a *communication channel*.

Consider subgraphs  $G_1$  and  $G_2$ . Color each vertex white if ultimately (according to the permutation that needs to be realized) we want to see it in  $G_1$  and black if we want to see it in  $G_2$ . The task is to permute the colors by swapping colors in the adjacent vertices such that all white colored vertices go to the  $G_1$  part and all black ones move to  $G_2$ . The bottleneck is in how many edges join the two halves  $G_1$  and  $G_2$ —the number of such edges represents the *carrying capacity* of the communication channel. This is because all white elements from  $G_2$  and all black elements from  $G_1$  must, at some point, use one of such communication channels to move to their subgraph.

If all colored vertices can be brought to their subgraph with a linear cost,  $a * n$ , then we iterate the algorithm and have the following figure for the complexity of the entire algorithm:  $C(n) \leq a * n + C(\frac{n}{s+1})$ , where  $C(n)$  is the complexity of the algorithm for a size  $n$  problem. The solution for such a recurrence is  $C(n) = \frac{a(s+1)n}{s}$ . If the graph has separability factor  $s = 1/2$ , the recurrence can be rewritten as  $C(n) \leq a * n + C(2n/3)$ . The latter has solution

$$C(n) = 3an + \text{const}, \quad (1)$$

providing a linear upper bound for the entire algorithm.

We next discuss how to move all white vertices into the  $G_1$  subgraph and, simultaneously, black ones into the  $G_2$  subgraph in linear time  $a * n$ . Consider a single subgraph, let us say  $G_1$ , and the edge(s) of  $G$  that we cut to create  $G_1$  and  $G_2$ . First, let us bring all black vertices as close to the communication channel as possible. To do so, we suppose that the communication channel consists of a single edge, otherwise, choose a single edge. We next cut all loops in  $G_1$  such that in the following solution we will not allow swapping values across all possible edges. After this is done, we have a rooted tree with the root being the unique vertex that belongs to  $G_1$  and is the end of the communication channel. A rooted tree has a natural partial order to its vertices, induced by the minimal length path from a given vertex to the root.

We next apply the following algorithm. Suppose  $G_1$  has  $k + 1$  vertices. At step  $i = 1..k$ , we look at vertices at depth  $k - i$  and their parent at depth  $k - i - 1$ . If the vertex at depth  $k - i$  is black and its parent is white, we call such a parent a *bubble* and interchange it with the child through applying a SWAP. We also look at all bubbles introduced on the previous steps. If a bubble has a black child, we SWAP the two (propagate the bubble). Otherwise, all children of the bubble are white, and as a result, this vertex is no longer a bubble. Let us note that once a bubble started “moving”, it will move each step of the algorithm until it is no longer a bubble, which happens only when all its children are white. By the step  $i = k$  all potential bubbles have started moving or have already finished their trip. It may take an additional  $k$  steps for moving bubbles to finish their movement. By the time step  $i = 2k$  is completed, every path from a vertex in  $G_1$  to the root will change color at most once (if color changes it can only change from white to black).

This brings us to the next part: interchanging white and black nodes in  $G_1$  and  $G_2$  and actually using the communication channel. We use the communication channel every odd step in this part of the algorithm to bring a single black vertex from  $G_1$  over to  $G_2$  and a single white vertex from  $G_2$  to  $G_1$ . Once a white vertex arrives in  $G_1$  we call it a bubble and rise it until all its children are white. A similar operation is performed with graph  $G_2$ . Every even step the root vertex of  $G_1$  is white (and thus is a bubble) and one of its children is black (if all children are white, the algorithm is finished;  $G_1$  is guaranteed to contain only white vertices, and all of them). We propagate the bubble to one of its children to have a black vertex ready for the next transfer. To get all white nodes to their side we will need at most  $2k$  swaps ( $k$  because there cannot be more than  $k$  white nodes missing, and  $*2$  because we use communication channel every second time).

Thus, the total cost of bringing white nodes to  $G_1$  and black ones to  $G_2$  is  $2k + 2k = 4k$ . Since in the graphs we consider  $s \geq 1/2$ , the above expression gives an upper bound of  $a = 8/3$ . Substituting this into the recurrence solution (1) gives the upper bound of  $8n + \text{const}$  for the number of levels in a quantum circuit composed with SWAPs working with the fastest interactions and realizing a given permutation. By considering permutation

$(n, 2, 3, \dots, n-1, 1)$  and the chain nearest neighbor architecture we can show that the above algorithm is asymptotically optimal.

**Physical interpretation.** The above formulated algorithm can be interpreted in terms of elementary physics. One can think of a graph as a container with a rather unusual shape (whatever the shape of the graph is when it is drawn), black nodes contain liquid, white nodes—air, and edges are tubes joining the containers. Part  $G_1$  is solely on the left and  $G_2$  on the right, so they are well separated in space. In other words, we have a mixture of air and water in some container. We next flip the container such that the  $G_1$  part comes on top and  $G_2$  is on the bottom. We then observe how the water falls down while the air bubbles rise up. Intuition tells us that the water will flow through the communication channel between  $G_1$  and  $G_2$  with some constant rate (ignore the pressure, friction and other physical parameters), so that the water will end up on the bottom in a linear time. Our algorithm tries to model this situation to some extent, however, to have an easier mathematical proof of linearity we block the communication channel for some time. In our implementation of the above algorithm, we do not block the communication channel in hopes of achieving a faster solution. We illustrate how this algorithm works with the following example.

**Example 4.** Consider trans-crotonic acid, which could be used as an environment for up to a 7-qubit computation. The values of qubits are stored in magnetic spins of carbon nuclei  $C_1, C_2, C_3$  and  $C_4$ , hydrogen nuclei  $H_1$  and  $H_2$  and the set of three (practically indistinguishable) hydrogens called  $M$ . This molecule is illustrated in Figure 3. We first cut the graph of chemical bonds into two maximally balanced graphs in terms of the equality of the number of nuclei used in the quantum computation. This is done via cutting across “cut 1” (shown in the Figure 3). Let the component on the left be called  $G_1$  and the component on the right be called  $G_2$ . Next, each of the two connected components is cut into two maximally balanced components. Graph  $G_2$  has three vertices and must be cut into two connected graphs. This necessitates that one of the components will have twice as many vertices as the other, and thus  $s = 1/2$ . The third and final cutting is trivial.

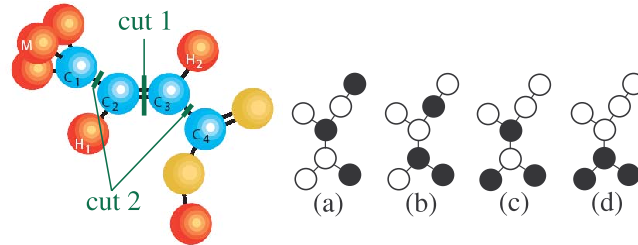


Figure 3: Left: Cutting the graph of chemical bonds (fastest interactions) for the trans-crotonic acid into connected subgraphs. The minimal value of  $s$  equals  $1/2$ . Right: Permuting values stored in spin-1/2 nuclei used in quantum computation.

Suppose we want to realize permutation

$$\begin{pmatrix} M & C_1 & H_1 & C_2 & C_3 & H_2 & C_4 \\ C_1 & C_2 & C_3 & C_4 & H_2 & H_1 & M \end{pmatrix}.$$

Following our water and air metaphor discussed previously, the vertices contain Water–Air–Water–Air–Air–Air–Water. Once the graph has been cut into the subgraphs as discussed, we turn the entire graph (i.e. container) 90 degrees clockwise (as illustrated in Figure 3(a)) and observe how the water falls down. First, the vertices  $M$  and  $C_1$  and, at the same time,  $C_2$  and  $C_3$ , exchange their content leading to Air–Water–Air–Air–Water–Water–Air, Figure 3(b). In the second step, the contents of  $C_1$  and  $C_2$  and, at the same time  $C_3$  and  $C_4$ , are interchanged leading to Air–Air–Air–Water–Water–Air, Figure 3(c). Finally, the contents of  $C_2$  and  $C_3$  are interchanged leading to Air–Air–Air–Air–Water–Water–Water (Figure 3(d)), meaning that all vertices that were desired in  $G_1$  are now moved to  $G_1$ , and also all vertices that we wanted to see in  $G_2$  are now located in  $G_2$ . At this step the problem falls into two completely separate components that can be handled in parallel: permute values in a connected graph with 4 vertices and a connected graph with 3 vertices.

Circuit name	# gates	# qubits	Environment name	# qubits	Estimated circuit runtime	Search space size
err. corr. encod. [12], Figure 2	9	3	acetyl chloride [12], Figure 1	3	.0136 sec	6
5 bit err. corr. ([10], Fig. 1)	25	5	trans-crotonic acid ([10], Fig. 3)	7	.0779 sec	2,520
pseudo-cat state prep. ([16], Fig. 1)	54	10	histidine ([16], Fig. 2)	12	.5170 sec	239,500,800

Table 2: Mapping experimentally constructed circuits into their physical environment.

### 5.3 Implementation and its scalability

We implemented the above algorithms in C++ using the VFLib graph matching library [19]. The bottleneck of our algorithm and its implementation is the efficiency of computing a solution to the subgraph monomorphism problem. This is because in order to solve the placement problem for a circuit with  $k$  gates, among which  $s$  are two-qubit gates, the subgraph monomorphism routine is called  $s$  times. All other operations performed by our algorithm and its implementation are at most quadratic in  $k$ .

The efficiency of the VFLib graph matching implementation was studied in [3]. The authors of [3] indicate that the implementation is sufficiently fast for alignment of graphs containing up to 1000 (and sometimes up to 10,000) nodes. A study of runtime for aligning a particular type of graphs with around 1000 vertices showed that the alignment took close to one second on average [3]. We thus conclude that our implementation should not take more than an hour (3600 seconds, in other words, 3600 calls to subgraph isomorphism subroutine) to place quantum circuits built on a few hundred qubits and containing a few thousand gates. At the present moment, such circuits are far in the future.

## 6 Experimental results

In this section we present two types of experiments. First, we take circuits that were executed experimentally on an existing hardware. We erase the placement assignment of the circuit qubits into the physical environment and try to reconstruct it. Our tool finds the best solutions found by hand by experimentalists (meaning the tool creates only one workspace and the matching made is equivalent to that by experimentalists). Table 2 summarizes the results. The first three columns list properties of the circuit—a short description of what the circuits does and its source, the number of gates and qubits in it. The next two columns present properties of the environment—the name of the environment and its source, and the maximal number of qubits it supports. The *Estimated circuit runtime* column shows a result of the running time our algorithm formulated—an estimate (actual runtime, depending on the particulars of technology, may be slightly different to account for the second order effects) of how long it will take to execute a given circuit. We do not list the actual mapping, because it is equivalent to that by the experimentalists [10, 12, 16]. The last column presents the size of the search space for placing a circuit as a whole (considering  $k$  subcircuits results in power  $k$  blow up of the search space size).

We next consider a circuit ([17], page 219) for a 6 qubit Quantum Fourier Transformation (QFT) and map it into a 7-qubit molecule. Unlike previous circuits considered in this paper the QFT circuit is not composed of liquid NMR primitives. This circuit is inconvenient for quantum architectures since it contains a 2-qubit gate for every pair of qubits. It cannot be executed in a chain nearest neighbor sub-architecture [6] since the longest spin chain in trans-crotonic acid has only five qubits. The circuit for 6-qubit QFT is used for the study of the relation between the value of *Threshold*, the number of subcircuits our software aligns individually and the overall cost of the alignment. Results are illustrated in Table 3, with the *Threshold* value appearing in the first column, the number of individual subcircuits aligned in second column, the time spent by the mapped circuit swapping qubits and the actual computation in the third and fourth columns, and the total cost of the alignment in the last column. As expected, usage of a large *Threshold* value resulted in a single working space, with the time spent on useful calculations decreasing when reducing the value of *Threshold*. However, the number of individually aligned

subcircuits grows, and the time spent in swapping the values increases. For *Threshold* value 50 (in this case, adjacency graph of the molecule is unconnected, which, in fact, is an indication that the value of *Threshold* is already too small), the mapped circuit does too much swapping, resulting in high overall cost. The best result is achieved with *Threshold* = 200. This indicates that the *quantum circuit placement tool has to use some rounds of SWAPs to achieve best results*. This is because the circuit with *Threshold* value 10000 is placed optimally as whole (i.e. when no SWAPs are allowed). The time spent in swapping suggests that our next goal should be the optimization of the swapping algorithm and the relation between time spent in swapping and doing useful calculation.

<i>Threshold</i>	Subcirc	SWAP	Compute	Total
10000	1	0 sec	.4137 sec	.4137 sec
1000	2	.2460 sec	.1949 sec	.4409 sec
500	5	.4398 sec	.0327 sec	.4725 sec
200	5	.3324 sec	.0298 sec	.3622 sec
100	5	.4515 sec	.0321 sec	.4836 sec
50	9	.6846 sec	.0201 sec	.7048 sec

Table 3: Relation between *Threshold*, number of subcircuits, and the cost of the alignment.

## 7 Conclusions

In this paper we presented an algorithm for the quantum circuit placement problem and its implementation. We tested our implementation on experimental data and computed, within a fraction of a second, the best results that have been reported by physicists. Further analysis indicates that our tool can handle very large quantum circuits (hundreds of qubits and thousands of gates) in a reasonable time (hours). We found that considering subcircuits and swapping their mappings is essential in achieving the best results. Our future work will be dedicated towards optimizing swapping circuits (in particular, we plan to explore look-ahead and peep-hole optimization techniques), study of the trade-off between increasing the size of the working space  $C$  and reducing SWAPs, and running larger (artificial) experiments to further address efficiency and scalability of our approach.

## Acknowledgements

We wish to acknowledge help of S. Aaronson from the University of Waterloo in proving NP-Completeness of the simplified version of the circuit mapping problem. This work was supported by NSERC, DTO-ARO, CFI, ORDCF, CIAR, CRC, ORF, and Ontario-MRI.

## References

- [1] M. D. Bowdrey, J. A. Jones, E. Knill, and R. Laflamme. Compiling gate networks on an Ising quantum computer. *Physical Review A*, 72(032315), 2005, quant-ph/0506006.
- [2] D. Copsey, M. Oskin, F. Impens, T. Metodiev, A. Cross, F. T. Chong, I. L. Chuang, and J. Kubiatowicz. Toward a scalable silicon-based quantum computing architecture. *IEEE J of Selected Topics in Quantum Electronics*, 9(6):1552–1569, 2003.
- [3] L. P. Cordella, P. Foggia, C. Sansone, and M. Vento. Performance evaluation of the VF graph matching algorithm. *10th ICIAP*, vol. 2, pages 1038–1041, 1999.
- [4] D. G. Cory, R. Laflamme, E. Knill, L. Viola, T.F. Havel, N. Boulant, G. Boutis, E. Fortunato, S. Lloyd, R. Martinez, C. Negrevergne, M. Pravia, Y. Sharf, G. Teklemariam, Y. S. Weinstein, and W.H. Zurek. NMR based quantum information processing: achievements and prospects. quant-ph/0004104, April 2000.

- [5] H. K. Cummins, C. Jones, A. Furze, N. F. Soffe, M. Mosca, J. M. Peach, J. A. Jones. Approximate quantum cloning with nuclear magnetic resonance. *Physical Review Letters*, 88:187901, 2002, quant-ph/0111098.
- [6] A. G. Fowler, S. J. Devitt, and L. C. L. Hollenberg. Implementation of Shor's algorithm on a linear nearest neighbor qubit array. *Quantum Information and Computation*, 4(4):237–251, 2004, quant-ph/0402196.
- [7] H. Häffner, W. Hänsel, C. F. Roos, J. Benhelm, D. Chek-al-kar, M. Chwalla, T. Körber, U. D. Rapol, M. Riebe, P. O. Schmidt, C. Becher, O. Gühne, W. Dür, and R. Blatt. Scalable multiparticle entanglement of trapped ions. *Nature* 438:643–646, December 2005, quant-ph/0603217.
- [8] R. Hughes *et al.* Quantum Computation Roadmap, July 2004. [http://qist.lanl.gov/qcomp\\_map.shtml](http://qist.lanl.gov/qcomp_map.shtml)
- [9] J. A. Jones. NMR quantum computation: a critical evaluation. *Fortschr. Phys.* 48(9-11):909–924, 2000, quant-ph/0002085.
- [10] E. Knill, R. Laflamme, R. Martinez, and C. Negrevergne. Implementation of the five qubit error correction benchmark. *Physical Review Letters*, 86(5811), 2001, quant-ph/0101034.
- [11] E. Knill, R. Laflamme, R. Martinez, and C.-H. Tseng. An algorithmic benchmark for quantum information processing. *Nature*, 404:368–370, March 2000.
- [12] M. Laforest, D. Simon, J.-C. Boileau, J. Baugh, M. Ditty, and R. Laflamme. Using error correction to determine the noise model. *Physical Review A* 75(012331), 2007, quant-ph/0610038.
- [13] L. Lavagno, G. Martin, and L. Scheffer, editors. *Electronic Design Automation for Integrated Circuits Handbook*. CRC Taylor and Francis, 2006.
- [14] R. Van Meter and K. M. Itoh. Fast quantum modular exponentiation. *Physical Review A*, 71(052320), May 2005, quant-ph/0408006.
- [15] R. Van Meter and M. Oskin. Architectural implications of quantum computing technologies. *ACM Journal on Emerging Technologies in Computing Systems*, 2(1):31–63, 2006.
- [16] C. Negrevergne, T. S. Mahesh, C. A. Ryan, M. Ditty, F. Cyr-Racine, W. Power, N. Boulant, T. Havel, D. G. Cory, and R. Laflamme. Benchmarking quantum control methods on a 12-qubit system. *Physical Review Letters*, 96(170501), 2006, quant-ph/0603248.
- [17] M. Nielsen and I. Chuang. *Quantum Computation and Quantum Information*. Cambridge University Press, 2000.
- [18] P. W. Shor. Polynomial-time algorithms for prime factorization and discrete logarithms on a quantum computer. *SIAM Journal of Computing*, 26:1484–1509, 1997, quant-ph/9508027.
- [19] Intelligent Systems and Artificial Vision Lab. The VFLib graph matching library. <http://amalfi.dis.unina.it/graph/>, 2006.